Carbon 104 (2016) 196–202

Contents lists available at ScienceDirect

Carbon

journal homepage: www.elsevier.com/locate/carbon

A generic approach for mechano-chemical reactions between carbonnanotubes of different functionalities

Mohamad A. Kabbani [a, *], Chandra Sekhar Tiwary [a], Anirban Som [b, 1], K.R. Krishnadas [b, 1], Pedro A.S. Autreto [a, c, e], Sehmus Ozden [a], Kunttal Keyshar [a], Ken Hackenberg [a], Alin Christian Chipara [a], Douglas S. Galvao [c], Robert Vajtai [a], Ahmad T. Kabbani [d], Thalappil Pradeep [b, **], Pulickel M. Ajayan [a, b, ***]

[a] Department of Materials Science and Nano Engineering, Rice University, Houston, TX, 77005, USA
[b] DST Unit of Nanoscience and Thematic Unit of Excellence, Department of Chemistry, Indian Institute of Technology Madras, Chennai, 600 036, India
[c] Applied Physics Department, State University of Campinas, Campinas, SP, 13083-959, Brazil
[d] Natural Science Department, Lebanese American University, Beirut, 1102 2801, Lebanon
[e] Universidade Federal do ABC, Santo André-SP, 09210-580, Brazil

ARTICLE INFO

Article history:
Received 11 December 2015
Received in revised form
25 February 2016
Accepted 28 February 2016
Available online 16 March 2016

ABSTRACT

Here, we report similar reactions between nanotubes carrying functionalities, namely carbon nanotubes (CNTs) with the acyl chloride/hydroxyl and amine/carboxylic functionalities directly attached to their surfaces, resulting in the formation ofchemically modified graphene products. The reaction is spontaneous and is facilitated by simple grinding of the reactants. The new solid-state reactions have been confirmed using different spectroscopic and electron microscopy techniques.

1. Introduction

Nanoscale materials are attractive due to their unique size, large surface area, chemical and physical properties. Great advancements have been made in the last decade in the synthesis of nanoparticles, which led to new innovative applications in various fields such as catalysis, chemical sensing, photonics, electronic devices and drug delivery [1–8]. Although functionalization has been extensively used to overcome limitations, such as poor solubility, reactivity and processing, by conjugating these particles to different chemical moieties such as drug molecules, polymers or organic molecules, the reactions between differently functionalized nanoparticles have been given very little attention. Especially important, is how do the attributes of these particles reflect on the rate of the reaction and how do the nanoscopic reactivities compare to that of the bulk molecular one. The most remarkable chemical reaction reported between nanoparticles is the dimerization of fullerene molecules inside carbon nanotubes 'peapods' [9,10]. In this type of confinement reaction, the degrees of freedom are restricted to translational motion in one dimension. Encapsulation of the C_{60}s in the CNT peapod structure has been reported to cause a decrease of fullerenes intermolecular distance by 3–4% than in bulk crystals. Structure optimization techniques indicates that the net energy gain associated with the encapsulation of the C_{60}s gives rise to a capillary force with an effective pressure of the order of GPa that will give rise to a strain on the CNT wall. Other than the confinement peapod fullerene/CNT dimerization reaction, no reaction has been reported between nanoparticles of different functionalities. Although an abundance of both top-bottom and bottom-up synthetic strategies have evolved in the last decade for the production of graphene [11–25], none of them considered the solid-state reaction between CNTs of different functionalizations.

We have recently reported the unzipping of MWCNTs via a one-pot room temperature solid-state mechano-chemical reaction between MWCNT–COOH and MWCNT–OH. The reaction involves hydrogen bond mediated proton transfer step that is followed by two elimination steps: water condensation and decarboxylation [26]. To test this type of solid-statedouble eliminations scheme, we here, report two new modifications of mechano-chemical reactions

* Corresponding author.
** Corresponding author.
*** Corresponding author. Department of Materials Science and Nano Engineering, Rice University, Houston, TX, 77005, USA.
E-mail addresses: mak8@rice.edu (M.A. Kabbani), pradeep@iitm.ac.in (T. Pradeep), ajayan@rice.edu (P.M. Ajayan).
[1] Equal contribution.

http://dx.doi.org/10.1016/j.carbon.2016.02.094
0008-6223/

of differently functionalized MWCNTs, namely MWCNT–COCl/MWCNT–OH and MWCNT–NH_2/MWCNT–OH reactions, Fig. 1.

Reactions are facilitated by manual grinding of equal weights of the functionalized CNTs as described in our previous report [26]. The two new modifications together with the previously reported one are summarized in equations (1)–(3) [26]

$$\text{MWCNT–COOH} + \text{MWCNT–OH} \rightarrow G + G' + CO_2 + H_2O \quad (1)$$

$$\text{MWCNT–}NH_2 + \text{MWCNT–COOH} \rightarrow G + G' + NH_3 + CO_2 \quad (2)$$

$$\text{MWCNT–COCl} + \text{MWCNT–OH} \rightarrow G + G' + CO_2 + HCl \quad (3)$$

G and G'are the graphene types derived from the two differently functionalized CNTs.

In reaction 2, the unzipping double elimination is mediated by hydrogen-bond formation, followed by proton transfer from the COOH group to the NH_2, double elimination of NH_3 and CO_2, formation of CNTs ion pair and consequent unzipping of CNTs by the heat of the exothermic reaction [26], while the double elimination in reaction 3 proceeds via the condensation of HCl, decarboxylation, CNTs ion pair formation and CNTs unzipping [26]. Each of the above reaction can be considered as a double elimination reaction as summarized in Table.1. Graphene products as well as the double elimination products of the new mechanochemical modifications are confirmed using spectral techniques and electron microscopy ones.

Table 1
Different modifications of the mechanochemical reaction between differently functionalized MWCNTs.

Reaction	Types of elimination
1	Water condensation + decarboxylation
2	Dehydroamination + decarboxylation
3	Dehydrochlorination + decarboxylation

2. Results and discussion

ATR-IR of the solid-state reaction product in the reaction mixture MWCNT–COOH/MWCNT–NH_2 (Fig. 2a), reveals almost complete absence of the strong doublet band at about 3000 cm^{-1}due to the N–H stretching mode as well as absence of broad bands in the region 2500–3000 cm^{-1}due to O–H stretching in the MWCNT–COOH/MWCNT–NH_2 mixture in agreement with water and ammonia condensation reaction. Also, the intensity of the band at 1680 cm^{-1} due to the carbonyl band of the carboxylic group diminishes significantly with appearance of the adsorbed

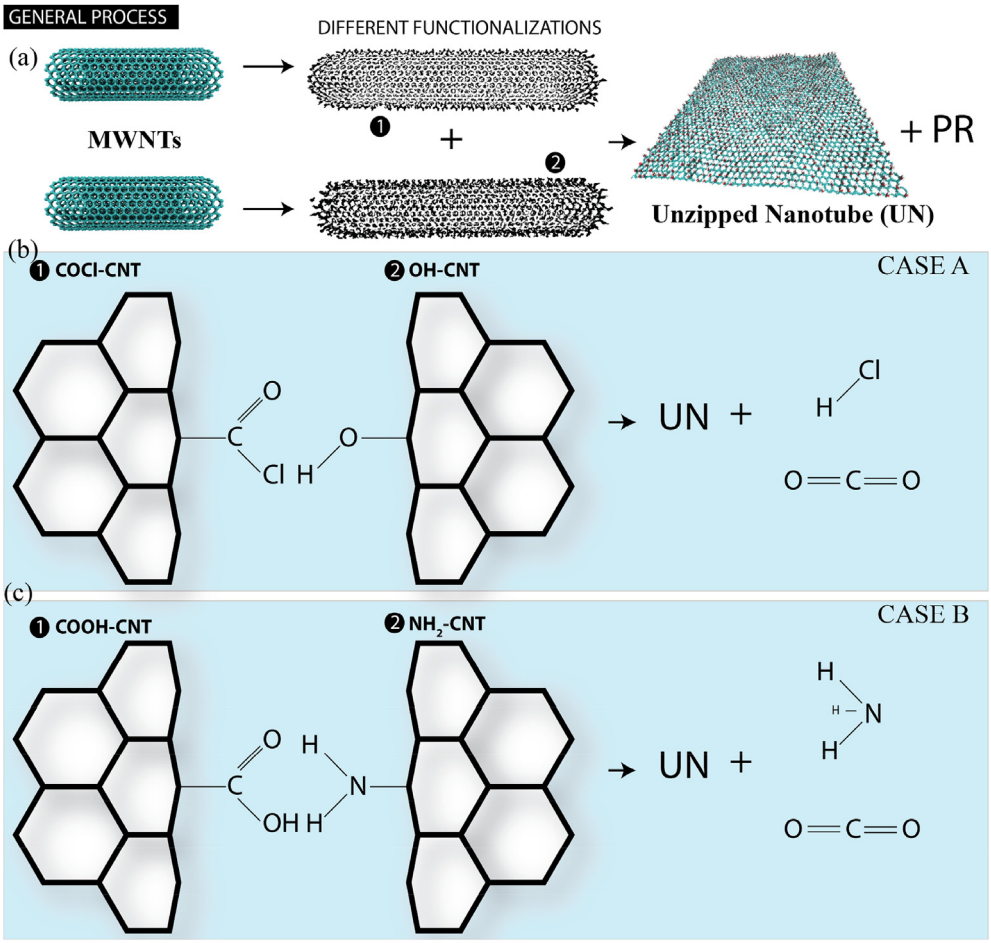

Fig. 1. (**a**) General solid-state unzipping reaction of differently functionalized CNTs. (**b**)Unzipping double elimination reaction between MWCNT–COCl and MWCNT–OH: First elimination leads to the condensation of HCl, which is followed by decarboxylation, formation of CNTs ion pair and consequent unzipping of CNTs by the heat of the exothermic reaction. (**c**) Unzipping double elimination reaction between MWCNT–COOH and MWCNT–NH_2 is mediated by hydrogen-bond formation, followed by proton transfer from COOH to NH_2, formation of the NH_3 and CO_2, formation of CNTs ion pair and consequent unzipping of the CNTs by the heat of the exothermic reaction. (A color version of this figure can be viewed online.)

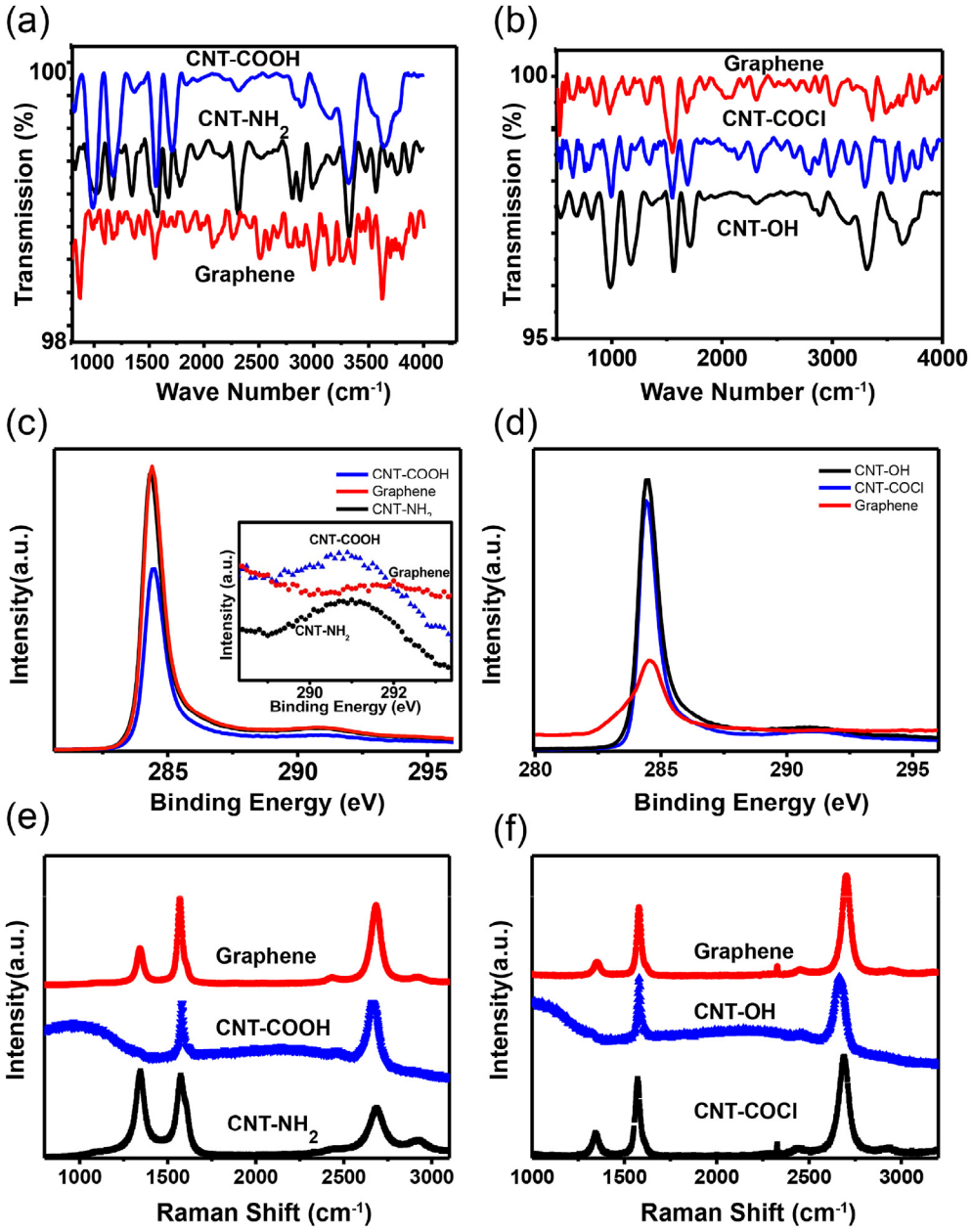

Fig. 2. (**a**)ATR-IR of reactants and products in the solid-state reaction of MWCNT−NH_2 and MWCNT−COOH. Both the doublet band due to NH_2 at about 3000 $cm^{-1}$and broad band in the 2500−3000 cm^{-1} region due to the stretching O−H mode are absent in the reaction product in support of the elimination of CO_2 and NH_3.(**b**) ATR-IR of reactants and products in the solid-state reaction of MWCNT−OH and MWCNT−COCl. The conjugated carbonyl band at about 1750 cm^{-1} and broad band of the O−H mode is absent in the product in support of HCl and CO_2 elimination. C=C band in the graphene product becomes dominant. (**c**–**d**) C1s XPS of reactants and products in the reactive combinations of MWCNT−NH_2/MWCNT−COOH (c), and MWCNT−OH/MWCNT−COCl (d). The signal at 289.2 eV due to the carbonyl group in both combinations disappears upon grinding of CNTs and is dominated by the C=C signal of graphene at 284.6 eV.The higher intensity of the latter band in the NH_2/COOH combination is compatible with the bigger yield of this combination relative to the COCl/OH combination. (**e**–**f**) Raman spectra of MWCNT−NH_2/MWCNT−COOH, (e), and MWCNT−OH/MWCNT−COCl, (f). The G, D and 2Dbands are all blue shifted in the graphene product relative to those of CNTs. (A color version of this figure can be viewed online.)

CO_2 and NH_3 bands at 2370 and 3510 cm^{-1}, respectively [27]. Compatible with this conclusion is the disappearance of the two strong bands due the C−N stretching in the region 1180–1360 cm^{-1} mode and absence the broad band at about 900 cm^{-1} due to N−H bending in the graphene product of the reaction. Similarly, the conjugated carbonyl band of the acyl chloride at 1750 $cm^{-1}$and broad OH stretching bands of the CNT are almost absent in the product of the solid−state reaction of MWCNT−COCl and MWCNT−OH with the C=C band at 1600 cm^{-1} of the graphene becoming dominant (Fig. 2a–b).

Table 2
Yield and $I_{2D}/1_G$ ratios of the graphene obtained via reactions of different functionalities CNTs.

Solid-state reaction	Yield	I_{2D}/I_G
−COOH/OH (1)	60%[26]	1.20
−COOH/NH_2 (2)	75%	0.95
−COCl/OH (3)	71%	2.10

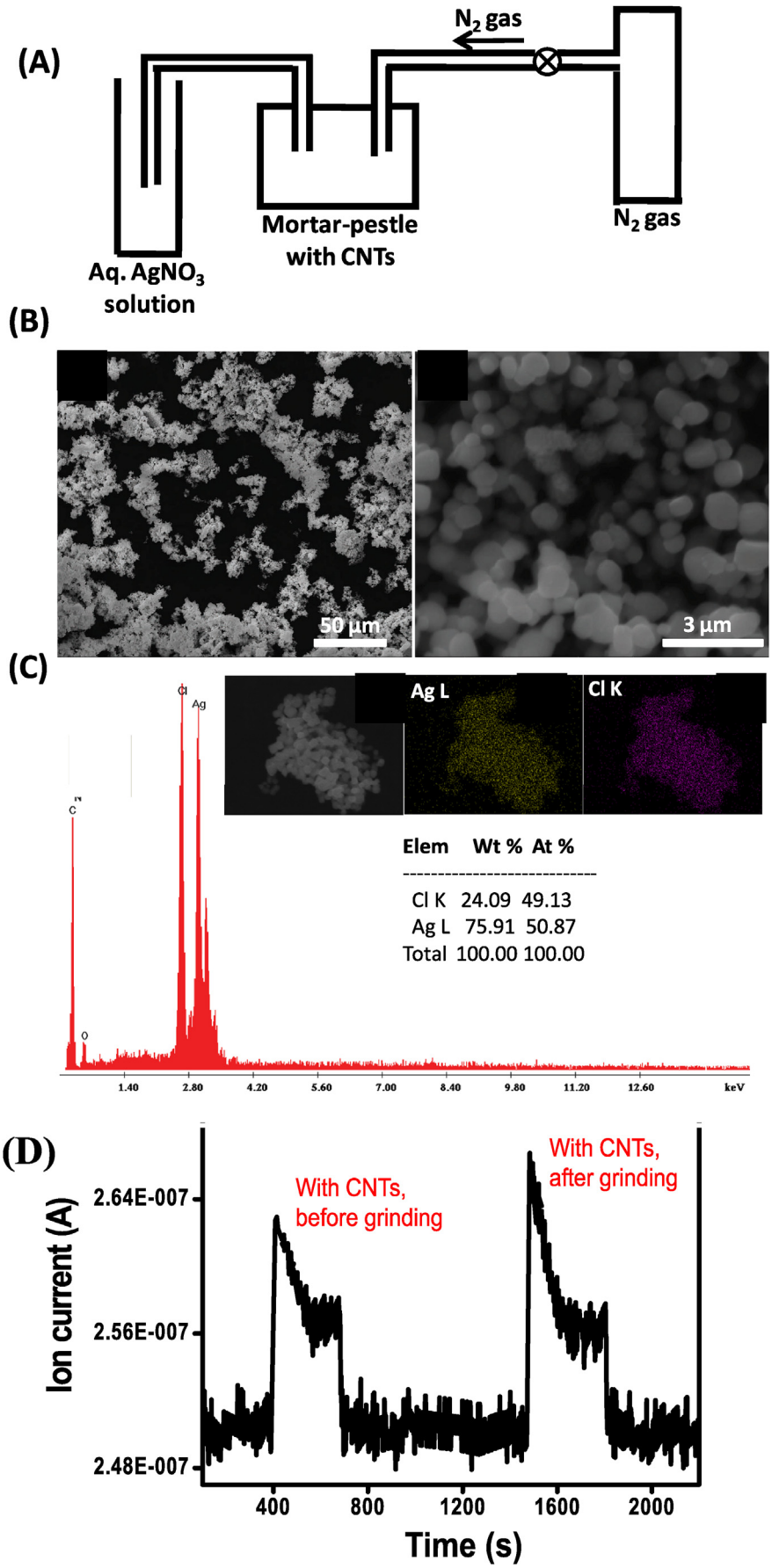

Fig. 3. A simple schematic of the experimental set up used for the detection of evolved HCl gas (A), SEM images of the lumps of AgCl particles formed at low magnification and high magnification (B), EDAX data of the AgCl formed (C). The Inset shows the SEM image of one of the lumps of AgCl formed, and elemental mapping of the same lump collecting the intensities of Ag L and Cl K. Ion current vs. time plots for NH_3^+ obtained during the solid-state condensation reaction between $-COOH$ and $-NH_2$ functionalized CNTs (D). (A color version of this figure can be viewed online.)

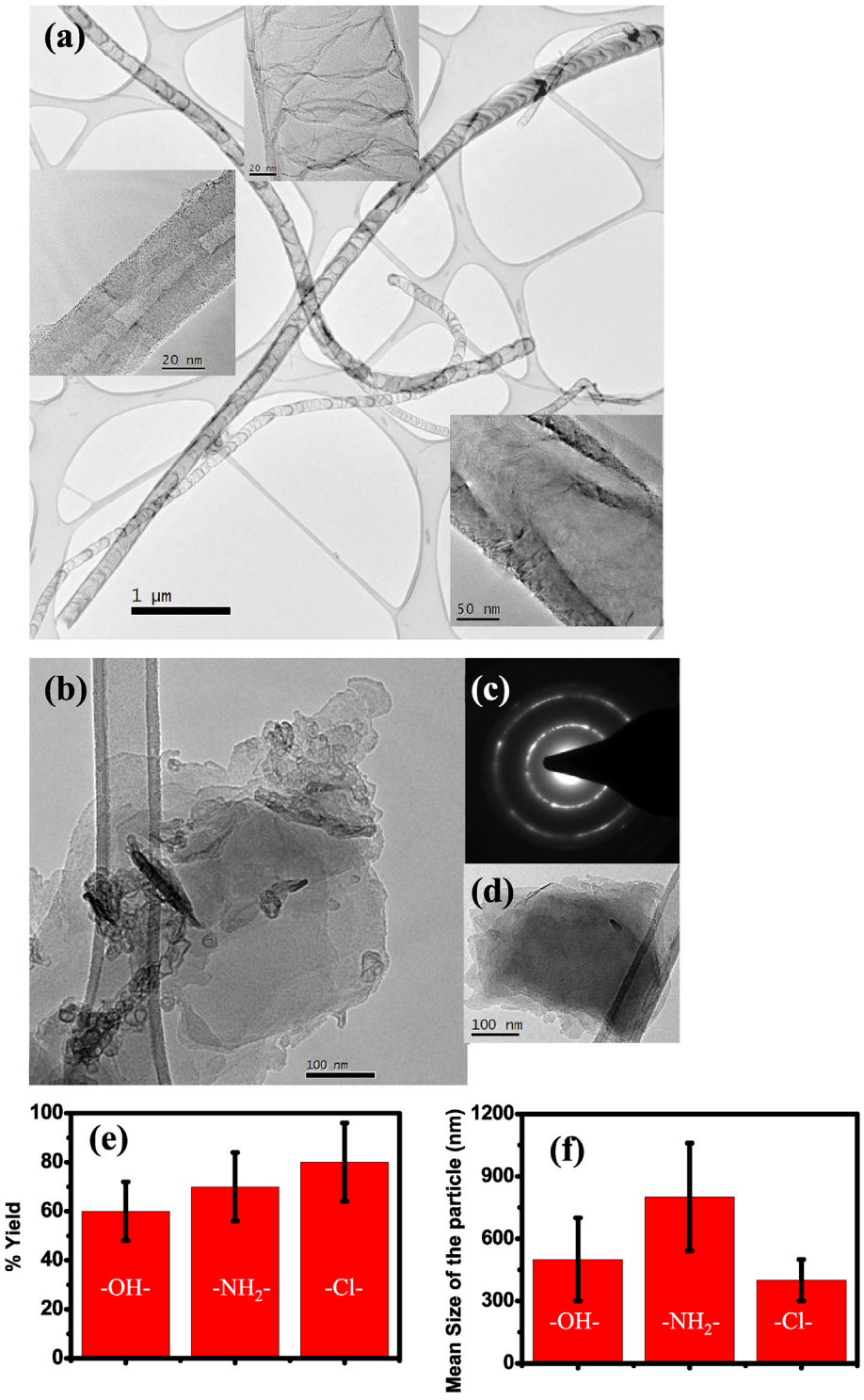

Fig. 4. (**a**) Low magnification bright field TEM image of multiwalled CNTs, high magnification images revealing number of walls shown in the inset. (**b**) Low magnification bright field image of graphene produced after reaction (**c**) SAD pattern from these products (**d**) The graphene produced during Cl functionalization (**e**) %yield produced in OH, NH_2 and Cl functionalized using current work (**f**) Size of particle produced in current methods. (A color version of this figure can be viewed online.)

In the C1s XPS of the MWCNTs, the signal at 291 eV due to the carbonyl group of the *acyl* and carboxylic MWCNTs disappears upon grinding while the signal at 284.6 eV (Fig. 2c–d) due to C=C becomes the dominant signal [28]. This is strong evidence in favor of graphene formation and therefore doubles condensation reactions in the MWCNTCOCl/MWCNT–OH and MWCNTNH_2/MWCNT–COOH reactive mixtures. In addition, according to XPS, chlorine content in reaction 3 drops from 0.195% before grinding to 0.056% in the graphene product giving rise to a yield of about 70%.This is accompanied by a drop in the oxygen content from 0.304 in the reaction mixture to 0.132% (XPS data, Supplementary Table 1). In the MWCNTNH_2/MWCNT–COOH nitrogen content drops from 0.300% in the amine CNT to 0.0375% in the graphene product-giving rise to 75% yield reaction.

Raman spectroscopy is a quick, easy and powerful tool that can be used for structural as well as quality characterization of the graphene products in the mechanochemical reactions. The intensity ratio of the D and G bands, $I_D/I_{G,\ is}$ commonly used to evaluate the quality of the graphene material. The I_D/I_G for the graphene products are 0.23 and 0.41 for the MWCNTCOCl/MWCNT−OH and MWCNTCOOH/MWCNT−NH_2 combinations respectively, Fig. 2e–f. The low value of the graphene due to the graphene product in the former is consistent with 1–3 layers graphene quality obtained via the CVD method where the upper limit of I_D/I_G was found to be 0.3 [19]. This result is consistent with the I_{2D}/I_G ratio whose value of ~ 2 hallmarks the low layers graphene quality. On the other hand both ratios of I_D/I_G (0.41) and I_{2D}/I_G (0.95) for the graphene obtained via the NH_2/COOH are consistent with graphene of more than three layers graphene according to the CVD scale. The enhanced numbers of layers could be related to greater tendency for the NH_2 and COOH groups to hydrogen bond [29–32]. Yields of the graphene obtained via different solid-state reactions are summarized in Table 2.

In order to confirm the formation of HCl during the reaction between CNT-COCl and CNT-OH, the gaseous products formed during the grinding of these CNTs (in a mortar-pestle set up) were passed continuously into an aqueous $AgNO_3$ (10 mM) solution by using high pure N_2 (99.9%) as carrier gas. Schematic of is given in Fig. 3a. After 30 min of passing the gas mixture with continuous grinding, a white turbidity appeared in the $AgNO_3$ solution. This turbid solution was drop casted for SEM imaging (Fig. 3b) and EDAX elemental analysis (Fig. 3c), which showed the presence of AgCl particles confirming evolution of HCl gas in reaction between CNT-COCl and CNT-OH. A control experiment with only the CNT-COCl was conducted using the same set-up for which formation of AgCl was not observed.

As for reaction 3, evolution of gaseous ammonia during the reaction between −COOH and −NH_2functionalized MWCNTs was confirmed through a mass spectrometrometric detection procedure described in our earlier report [26]. In short, gaseous mixture formed during the grinding process was subjected to a Balzer Thermostar mass spectrometer and ion current corresponding to m/z 17 (corresponds to NH_3^+) was monitored. While an increase in the ion current was observed after mixing of the CNTs and subsequent sampling, similar increase was observed for other background gases like nitrogen and oxygen. But, sampling after the grinding the CNTs showed further increase in the ion current for NH_3 while increase in intensity for the background gases remained the same, proving formation of NH_3 (Fig. 3d). Fig. 3d, Ion current vs. time plots for NH_3^+ obtained during the solid-state condensation reaction between −OH and −$CONH_2$ functionalized CNTs.

The spectroscopic (Raman, FTIR and XPS) and mass spectral measurements are further confirmed using transmission electron microscopy. Fig. 4a shows bright field transmission electron microscope image of multi-walled carbon nanotubes used in current experiments. The diameter of these nanotubes varies from 40 to 100 nm with a number of walls varying from 6 to 12 and the length of the nanotubes are in the order of few microns. There is no observable change observed in the size and morphology of the tubes due to functionalization. Fig. 4b shows bright field image of product produced due to reaction of chloride and OH functionalized nanotubes. It shows graphene with irregular morphology along with part of unzipped carbon nanotubes. These are stacked on each other in different orientation as shown in Fig. 4c. On the other hand the bright field of NH_2 and OH functional CNT shows graphene with smaller size and less number of walls. We observe less untreated CNTs. Based on the imaging, we have calculated percentage of graphene observed. To gain more insight about the reactivates of different combinations, we have used microscopy to find the yield range and size observed of graphene obtained in the OH/−COOH, OH/−Cl and COOH/-NH_2combinations. The results are 40–60% [400 nm], 50–70% [800 nm] and 60–80% [400 nm] respectively as shown in Fig. 4e–f. The yield results are compatible with the XPS data as well as chemical reaction discussed before.

In light of the above and according to the mechanism reportedelsewhere for reaction 1, the hydrogen-bond mediated proton transfer step in reaction 2 is followed by the formation of MWCNT−NH_3^+/MWCNT−COO^-, loss of CO_2/NH_3, formation of CNTs ion pair and the unzipping processes [26]. Also, dehydrochlorination in 3 is followed by decarboxylation of an ester group connecting G and G′ leading to ion-pairs formation and consequently CNTs unzipping. The higher yield of graphene via the acyl chloride CNT reaction as compared to that obtained via the mechanochemical reaction of MWCNT−COOH and MWCNT−OH reported can be related to the high reactivity of the acyl chloride as compared to the carboxylic acid since the electron-withdrawing chlorine atom makes the carbonyl carbon more positive and therefore more susceptible to the attack by the hydroxyl group of MWCNT−OH. The higher yield in the −NH_2/−COOH reaction is due to the more exothermic proton transfer between the acidic carboxylic group and the basic amino group, a factor that will increase the % of broken C–C bonds in reaction 2 relative to that in 1 as we have confirmed in the detailed theoretical hot spots protocol of reaction 1 [33–38,26].

In conclusion, we have demonstrated the general case of a solid-state reaction between different functional groups covalently bound to carbon nanotubes that can be used to engineer different types of graphene. The exothermic reaction between these functionalities facilitated by simple mechanical grinding, results in bond breaking and the energy released in the process helps to break bonds and unzip the CNTs resulting in graphene. The hydrogen bond mediated proton transfer mechanism leading to the unzipping reaction of the MWCNTs can be used equally for different modifications of functional groups and therefore as a generic approach to develop synthetic frameworks for graphene productions such as doped graphene. The unzipping process is not accompanied by harsh physical and chemical techniques and accordingly can be used better in integration of graphene in electronic devices.

Author contributions

MK and ATK proposed the project. MK and CST designed and conducted experiments. AS, KRK, SO, KK, KH, ACC helped in characterization. AS, KRK performed and TP supervised the mass spectral measurements and TP proposed the mechanochemical name for the reaction. MK, CST, RV, TP, ATK and PMA analyzed the data and wrote the paper. All authors discussed and revised the final manuscript.

Competing financial interests

The authors declare no competing financial interests.

Acknowledgments

This work has been supported by U.S. Department of Defense: U.S. Air Force of Scientific Research for the Project MURI: “Synthesis and Characterization of 3-D Carbon Nanotube Solid Networks” Award No. FA9550-12-1-0035. Work at IIT Madras was supported by a grant through the Nano Mission, Government of India. Part of work was done while MAK was a visiting student at IIT Madras. CST would like to thank Indian Institute of Science, Bangalore for support. P.A.S.A., acknowledge financial support from the Brazilian

Agencies CNPq, CAPES, and FAPESP and also thank the Center for Computational Engineering and Sciences at Unicamp for financial support through the FAPESP/CEPID Grant 2013/08293-7.

Appendix A. Supplementary data

Supplementary data related to this article can be found at http://dx.doi.org/10.1016/j.carbon.2016.02.094.

References

[1] L. Vigdeman, E.R. Zubarev, Therapeutic platforms based on gold nanoparticles and their covalent conjugates with drug molecules, Adv. Drug Deliv. Rev. 65 (2013) 663–676.
[2] J.D. Gibson, B.P. Khanal, E.R. Zubarev, Paclitaxel–functionalized gold nanoparticles, J. Am. Chem. Soc. 129 (2007) 11653.
[3] B. Saha, J. Bhattacharya, A. Mukherjee, A. Ghosh, C. Santra, A. Dasgupta, P. Karmakar, *In vitro* structural and functional evaluation of gold nanoparticles conjugated antibiotics, Nanoscale Res. Lett. 2 (2007) 614–622.
[4] A. Rai, A. Prabhune, C.C. Perry, Antibiotic mediated synthesis of gold nanoparticles with potent antimicrobial activity and their application in antimicrobial coatings, J. Mater Chem. 20 (2010) 6789–6798.
[5] L. Wang, C. Zhu, X. Wei, X. Kan, Preparation and application of functionalized nanoparticles of CdS as a fluorescence probe, Anal. Chim. Acta 468 (2005) 35–41.
[6] R. Shenhar, T.B. Norsten, V.M. Rotello, Polymer-mediated nanoparticle assembly: structural control and applications, Adv. Mater. 17 (2005) 657–669.
[7] E.S. Jeng, A.E. Moll, A.C. Roy, J.B. Gastala, M.S. Strano, Detection of DNA hybridization using the near-infrared band-gap fluorescence of single-walled carbon nanotubes, Nano Lett. 6 (2006) 371–375.
[8] N.I. Kovtyukhova, T.E. Mallouk, L. Pan, E.C. Dickey, Individual single-walled nanotubes and hydrogels made by oxidative exfoliation of carbon nanotubes ropes, J. Am. Chem. Soc. 125 (2003) 9761–9769.
[9] B.M. Smith, M. Monthiooux, D.L. Luzzi, Encapsulated C60 in carbon nanotubes, Nature 396 (1998) 323–325.
[10] S.E. Zhu, F.L. Fei, G.W. Wang, Mechanochemistry of fullerene and related materials, Chem. Soc. Rev. 42 (2013) 7535–7570.
[11] K.S. Novoselov, et al., Electric field effect in atomically thin carbon films, Science 306 (2004) 666–669.
[12] M. Qian, et al., Formation of graphene sheets through laser exfoliation of highly ordered pyrolytic graphite, Appl. Phys. Lett. 98 (2011) 173108.
[13] G. Zhao, D. Shao, C. Chen, X. Wang, Synthesis of few-layered grapheme by hydrogen peroxide plasma etching of graphite, Appl. Phys. Lett. 98 (2011) 1831149.
[14] Y. Hernandez, et al., High-yield production of graphene by liquid-phase exfoliation of graphite, Nat. Nanotechnol. 3 (2008) 563–568.
[15] Wsh Jr., W.S.H.R.E. Offeman Jr., Preparation of graphite oxide, J. Am. Chem. Soc. 80 (1958), 1339–1339.
[16] D. Li, M.B. Muller, S. Gilje, R.B. Kaner, G.G. Wallace, Processable aqueous dispersions of graphene nanosheets, Nat. Nanotechnol. 3 (2008) 101–10517.
[17] S. Niyogi, et al., Solution Properties of graphite and graphene, J. Am. Chem. Soc. 128 (2006) 7720–7721.
[18] K.S. Kim, et al., Large-scale pattern growth of graphene films for stretchable transparent electrodes, Nature 457 (2009) 706–710.
[19] A. Reina, et al., Large area, few-layer graphene films on arbitrary substrates by chemical vapor deposition, Nano Lett. 9 (2009) 30–35.
[20] Y. Wu, et al., Efficient and large-scale synthesis of few-layered graphene using an arc-discharge method and conductivity studies of the resulting films, Nano Res. 3 (2010) 661–669.
[21] C. Berger, et al., Electronic confinement and coherence in patterned epitaxial graphene, Science 312 (2006) 1191–1196.
[22] J. Zhao, et al., An approach for synthesizing graphene with calcium carbonate and magnesium, Carbon 50 (2012) 4939–4944.
[23] A.C. Chakrabarti, Conversion of carbon dioxide to few-layer graphene, J. Mater. Chem. 21 (2011) 9491.
[24] J.M. Tour, et al., Longitudinal unzipping of carbon nanotubes to form graphene nanoribbons, Nature 458 (2009) 872–876.
[25] L. Jiao, L. Zhang, X. Wang, G. Diankov, H. Dai, Narrow graphene nanoribbons from carbon nanotubes, Nature 458 (2009) 877–880.
[26] M.A. Kabbani, et al., Ambient solid-state mechano-chemical reactions between functionalized carbon nanotubes, Nat. Commun. 6 (2015) 7291.
[27] D. Harris, M. Bertolucci, Symmetry and Spectroscopy, Dover Publications, New York, 1989.
[28] D. Yang, G. Guo, J. Hu, C. Wang, D. Jiang, Hydrothermal treatment to prepare hydroxyl group modified multi-walled carbon nanotubes, Mater. Chem. 18 (2008) 350–354.
[29] A.C. Ferrari, D.M. Basko, Raman spectroscopy as a versatile tool for studying the properties of graphene, Nat. Nanotechnol. 8 (2013) 235–246.
[30] A.C. Ferrari, et al., Raman spectrum of graphene and graphene layers, Phys. Rev. Lett. 97 (2006) 187401–187404.
[31] D. Graf, et al., Spatially resolved Raman spectroscopy of single and few layer graphene, Nano Lett. 7 (2007) 238–242.
[32] R. He, et al., Observation of low energy raman modes in twisted bilayer graphene, Nano Lett. 13 (2013) 3594–3601.
[33] J. Pauling, General Chemistry, third ed., Freeman, 1970, p. 913.
[34] R.P.B. Santos dos, E. Perim, P.A.S. Autreto, Brunetto, D.S. Galvão, On the unzipping of multiwalled carbon nanotubes, Nanotechnology 23 (2012) 465702.
[35] P. Jund, R. Jullien, Molecular-dynamics calculation of the thermal conductivity ofvitreous silica, Phys. Rev. B 59 (1999) 13707–13711.
[36] P. Chantrenne, J.L. Barrat, Finite size effects in determination of thermal conductivities: comparing molecular dynamics results with simple models, J. Heat. Transfer. 126 (2004) 577–585.
[37] Carbon Nanotubes: Advanced Topics in the Synthesis, Structure, Properties and Applications, Springer, 2008.
[38] M.A.J. Chen, H. Hamon, Y. Hu, A.M. Chen, PCEk Rao, R.C. Haddon, Science 282 (1998) 95.